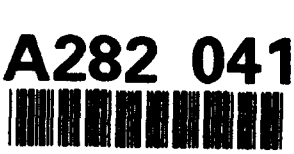

PL-TR-93-2192

THE DEVELOPMENT OF LABORATORY ION SOURCES FOR MASS SPECTROMETER CALIBRATION

J.M. CALO
W.D. LILLY

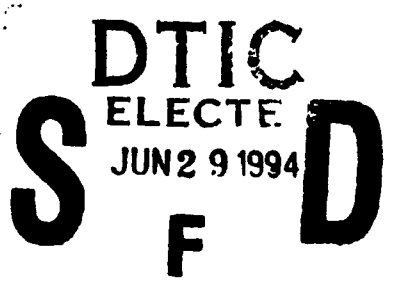

Brown University
Division of Engineering
Providence, RI 02912

August 1993

Final Report
Period Covered: 2 May 1991 - 3 August 1993

PHILLIPS LABORATORY
Directorate of Geophysics
AIR FORCE MATERIEL COMMAND
HANSCOM AIR FORCE BASE, MA 01731-3010

REPORT DOCUMENTATION PAGE

Form Approved
OMB No 0704-0188

1. AGENCY USE ONLY (Leave blank)	2. REPORT DATE	3. REPORT TYPE AND DATES COVERED
	August 1993	Final 2 May 1991 - 3 August 1993

4. TITLE AND SUBTITLE
The Development of Laboratory Ion Sources for Mass Spectrometer Calibration

5. FUNDING NUMBERS
PE 61102F
PR 2310 TA G3 WU BO

Contract F19628-91-K-0015

6. AUTHOR(S)
J. M. Calo
W. D. Lilly

7. PERFORMING ORGANIZATION NAME(S) AND ADDRESS(ES)
Brown University
Division of Engineering
Providence, RI 02912

PERFORMING ORGANIZATION REPORT NUMBER

9. SPONSORING / MONITORING AGENCY NAME(S) AND ADDRESS(ES)
Phillips Laboratory
29 Randolph Road
Hanscom AFB, Ma 01731-3010

Contract Manager: Donald Hunton/GPID

10. SPONSORING / MONITORING AGENCY REPORT NUMBER
PL-TR-93-2192

11. SUPPLEMENTARY NOTES

12a. DISTRIBUTION / AVAILABILITY STATEMENT

12b. DISTRIBUTION CODE

13. ABSTRACT *(Maximum 200 words)*

Electron impact ion sources were developed for the purpose of quadrupole mass spectrometer calibration in the laboratory. Prototype ion sources were constructed, and tested for operation in both positive and negative ion modes. In the positive ion mode, sensitivities approaching 10^{-3} A/torr were obtained at the highest filament currents tested. Ion currents were linear over an order of magnitude in pressure. Collected ion currents generally increased with electron energy, following somewhat the trend with total ionization cross section.

The results of energy analysis of the ion beams are consistent with Gaussian beams with relatively wide variances. Typical beam energies peaked in the regime of 30-35V, with variances of 17-18V. The ion beams did not appear to be fully accelerated at the analyzing electrode. The beams generally seemed to become more Gaussian with reduced variances at the lower electron energies.

The use of magnets did not noticeably improve ion source performance in the positive ion mode. However, it did eliminate a significant background current problem at the collector plate.

In the negative ion mode, total collected negative ion currents using SF_6 were approximately two orders of magnitude less than under comparable conditions in the positive ion mode.

14. SUBJECT TERMS
electron impact ion sources; positive and negative ions; mass spectrometry; ion beam energy analysis

15. NUMBER OF PAGES

16. PRICE CODE

17. SECURITY CLASSIFICATION OF REPORT	18. SECURITY CLASSIFICATION OF THIS PAGE	19. SECURITY CLASSIFICATION OF ABSTRACT	20. LIMITATION OF ABSTRACT
Unclassified	Unclassified	Unclassified	SAR

TABLE OF CONTENTS

LIST OF FIGURES

LIST OF TABLES

1.0. INTRODUCTION AND BACKGROUND

As part of its mission, the Ionospheric Interactions Branch of the Ionospheric Physics Division of the Phillips Laboratory has long had an ongoing program in mass spectrometric measurements of the ionosphere. The primary instruments employed for this purpose have been cryogenically pumped, quadrupole mass spectrometers. Over the years, various versions of these instruments have been flown on sounding rockets, satellites, and even balloon platforms (for lower altitude, stratospheric studies). These instruments have been used for ion (both positive and negative) and neutral composition measurements. Although many have been of either one type or the other, some have incorporated switched ion/neutral modes, and even switched positive/negative ion modes. The primary distinguishing characteristics of these instruments lies in these modes of operation. In the neutral mode, an (electron impact) ion source is used to generate the ions analyzed by the mass spectrometer from sampled neutral species, while in the ion modes no ion source is employed since the objective is to sample ambient ions from the atmosphere. However, no matter what the instrument type, all must be calibrated in the laboratory using standard ion sources in order that the signals obtained during flight may be interpreted on an absolute basis in terms of ambient species number densities. The primary objective of this contract was to develop laboratory calibration ion sources for these purposes.

The positive ion composition of the ionosphere is quite rich, involving species such as NO^+, O_2^+, N_2^+, O^+, N^+ the water cluster ion series $H_3O^+(H_2O)_n$, as well as other hydrated positive ions, meteoric metal ions, and many others (e.g., see Narcisi and Roth, 1970).

Negative ions have also long been known to be of considerable importance to

ionospheric chemistry. They are, of course, intimately related to local electron density, and interact with neutral species *via* their formation processes, as well as *via* ion-molecule reactions. Major ionospheric negative ion species include O^-, O_2^-, NO_2^-, NO_3^-, CO_3^-, CO_4^-, and heavy hydrated negative cluster ions such as $NO_3^-(H_2O)_n$, formed in the lower ionosphere (e..g, see Narcisi *et al.*, 1971).

Negative ions are also important in rocket release experiments of species with large electron attachment cross sections, such as SF_6. Such releases have been used to produce disturbances in the natural ionospheric plasma by creating "electron holes" (e.g., see Hunton *et al.*, 1987). In this latter work, a negative ion mass spectrometer was used to sample the the resultant negative ions over the altitude range 100-128 km. The major ions observed were SF_6^-, SF_5^-, F^-, and O^-. It is expected that species with high electron affinities will continue to be used for this purpose. Thus, it is essential to have well calibrated negative ion instruments to measure the effects of such releases.

Ionospheric composition and the relative abundances of these ionic species depend upon many variables such as altitude, sunlight, nighttime, season, latitude, naturally disturbed or undisturbed ionospheres, etc. In addition the ion chemistry and composition may be altered by intentional injections of other species. The positive and negative ion composition of the ionosphere is often a sensitive "fingerprint" of electrical, magnetic, and transport processes. Thus, mass spectrometric composition measurements represent a powerful tool for the investigation of the behavior of the ionosphere and how these phenomena affect Air Force communications, surveillance, and C^3I systems

Some of the upcoming missions involving mass spectrometer instruments include ion and neutral measurements aboard the Space Shuttle Orbiter. Such instruments were flown on STS-4 in 1982, STS-39 in 1991, and STS-46 in 1992;

and additional instruments are planned for flights in the future. At the Shuttle orbital altitudes in the upper ionosphere (e.g., 250-300 km), the major ambient positive ion is O^+. In addition to its intrinsic importance, O^+ can play a major role in interacting with the contaminant cloud which envelops the Orbiter (Hunton and Calo, 1985), as well as with exposed surfaces on the Orbiter leading to well-known material ablation phenomena and the "Shuttle glow" (e.g., see Mende *et al.*,1983). Therefore, mass spectrometric instruments intended for measurements aboard the Shuttle Orbiter should be calibrated with known fluxes of O^+, as well as with other expected positive ions.

This report summarizes the work that was done in the development of prototype laboratory sources for positive and negative ions to be used in the development of mass spectrometric instruments for experimental programs such as those mentioned above.

2.0. PROJECT WORK

2.1. General Support Apparatus.

All the ion source testing and development reported herein was performed on a conventional vacuum pump station serviced by a pumping stack consisting of a 4" Varian diffusion pump, a Granville-Phillips long life cryogenic trap, backed by an Alcatel vacuum pump.

The ion sources were mounted for testing on a standard 4.5 inch copper-gasketed flange with a 12-pin electrical feedthrough for supplying bias voltages and power to the ion source. The leads from the 12-pin connector were wired to a patch panel, which was in turn connected to the various power supplies. A rack of six 0-100V Kepco PCX100-0.2 MAT power supplies was used to supply most of the ion

source biasing potentials. A Kepco CK18-3 power supply was used to power the filament. Ion currents were measured with a Keithley 417 picoammeter.

2.2. Positive Ion Source.

2.2-1. Background.

Many techniques have been developed for the production of ions for mass spectrometric analysis. In addition to electron impact, these include photoionization, field ionization, spark and discharge sources, and chemical ionization techniques. However, the most versatile and widely used of all the techniques is undoubtedly electron impact.

The principal requirements for a laboratory calibration ion source include:

(1) production of a range of ion masses;

(2) high signal intensities;

(3) adjustable ion energies;

(4) adjustable/measurable ion fluxes of characterized spatial distribution;

(5) stable, long term operation;

(6) simplicity of installation and use.

Although some of the ionization techniques may be optimized for one or more of these requirements for a particular species, none is capable of meeting all the criteria as well as electron impact ionization. In addition, this has been the ion source type used for neutral mode operation of mass spectrometers by the Air Force. Therefore, this approach was the one selected for the current application.

2.2-2. Description of Prototype Positive Ion Source.

Detailed schematics of the two ion sources designed and constructed for this project are presented in Figures 1(a) and 2(a). Corresponding wiring diagrams are presented in Figures 1(b) and 2(b). There are actually only minor differences

between the two sources. Plate spacing and placement of the electron collector are identical for both sources. Changes in aperture diameters and the absence of grids in ion source #2 (except for the accelerator plate) were made to improve field penetration of the repeller and extractor potentials into the ion volume. Changes in feedthrough arrangement in ion source #2 were made to eliminate potential interference by the repeller leadwire bushing within the ion volume and to achieve more unioform lead spacing. All the experimental work reported herein was performed with ion source #1. The ion sources were constructed principally from 304 stainless "eV Parts" purchased from Kimball Physics, Inc., Wilton, NH. The part numbers for all the "eV Parts" used in the construction of the ion source are indicated directly on the figures.

The filament assembly consists of 1.27 cm length of tungsten/3% rhenium wire (0.015 cm diameter) spot-welded between two stainless steel posts mounted on a stainless steel holder/reflector assembly. Electrons are emitted from the tungsten filament upon passage of current through the wire. The filament was typically run at a voltage of 2.5V, drawing a current of 2.5A (Kepco CK18-3 power supply). The electrons emitted from the filament are accelerated through a potential difference applied between the filament and the ion volume. Since the ion volume potential was typically held constant, the electron energy was varied by setting the potential of the filament with respect to the ion volume with a separate power supply (Kepco ABC500).

The accelerated electrons are collimated into a narrow flat beam or sheet crossing the axis of the ion volume through a slit (1 x 18 mm) defined by two brackets located immediately in front of the filament. The slit is one of four parts which enclose and define the ion volume. Most of the electrons are collected by the electron collector plate which is biased positively with respect to the ion volume.

The calibration gas is leaked into the source using a variable leak valve (Granville-Phillips 202 series). Ions are formed by electron impact in the path of the electron beam within the ion volume region. These ions are extracted at a right angle to the electron sheet through the aperture plate. Ion extraction is effected *via* the combined action of an extractor plate, a focus plate and an accelerating/decelerating grid.

A repeller electrode was also provided to assist in extracting ions from the ion volume. However, in operation it was found that its use typically degraded rather than improved the performance of the ion source. In the positive ion mode the repeller was intended to be positively biased with respect to the ion volume to "repel" positive ions towards the aperture in the ion volume. However, it typically acted to decrease the positive ion current by drawing electrons from the beam to more inefficient regions of the ion volume. Therefore, it was ultimately biased at the same potential as the ion volume.

The extracted ions are finally collected on the ion collector plate, and the current recorded using a Keithley 417 picoammeter. Collection of the ions in this manner requires that the ion collector plate operate at a potential *ca.* zero volts with respect to the vacuum system. Therefore, the ion energy is determined by the potential difference applied to the ion volume with respect to the vacuum chamber. Consequently, operation as a positive ion source requires that the ion volume be biased positively with respect to the ion collector plate.

The abbreviations that are used herein to indicate the various ion source elements and potentials are defined in Table 1.

The effects of permanent magnets on the performance of the prototype ion source were also investigated in a series of tests which are discussed below. All the data reported with the magnets in place are specifically indicated as such.

2.2-3. Results and Discussion.

Three test gases were used with the ion source in the positive ion mode: Ar, N_2, and SF_6.

Nitrogen.

Figure 3 presents total collected positive ion current versus source pressure for N_2. As expected, the behavior is reasonably linear with pressure. The resultant sensitivity is 1.1 x 10^{-4} A/torr. Sensitivity could be improved by running the filament at a higher current. Typical ion current versus filament current data are presented in Figure 4. As shown, the sensitivity increases to about 3.5 x 10^{-4} A/torr at a filament current of 2.8A. However, in order to maximize filament life, it was decided to conduct most of the ion source tests at a nominal filament current of 2.5A.

The behavior of the total collected positive ion current versus electron energy is presented in Figure 5. On the same graph are plotted relative total ionization cross sections for nitrogen from Rapp and Englander-Golden (1965). Thus, it is clear that while the total collected ion current does generally increase with electron energy, the qualitative behavior cannot be completely accounted for by the variation of the total ionization cross section alone. Apparently, various ion source efficiencies control the collected ion current to a considerable degree.

Results of the behavior of the source with ion energy are presented in Figure 6. The shapes of the curves at the three different electron energies are suggestive of an ion beam with significant beam spread. These curves were analyzed in the following manner. If the beam is assumed to be Gaussian in shape then the ion current distribution is given by:

$$\phi(z) = (S_o/\sqrt{(2\pi)})\exp(-z^2/2) \qquad [1]$$

where:

$z = (v - v_m)/\sigma$

v = retarding grid potential, V

v_m = retarding grid potential at 50% beam intensity; i.e., the mean of the Gaussian beam, V

σ = variance of the beam, V

S_o = total beam current, A

This description of the beam results in the following expression for the total collected beam current as a function of the retarding grid potential:

$$I(z) = (S_o/2)[1 - \mathrm{erf}(z/\sqrt{2})] = (S_o/2)\,\mathrm{erfc}(z/\sqrt{2})] \qquad [2]$$

where:

$$\mathrm{erf}(t) = (2/\sqrt{\pi}) \int_o^t \exp(-x^2)\,dx \qquad [3]$$

The best fits to the data obtained using Eq. [2] are also presented in Figure 6. As shown, the fits are reasonable, although it appears that the beam is more Gaussian at the lowest electron energy of 70eV. The means and variances obtained for the best fits were:

E.E. = 70 eV; v_m = 22V; σ = 12V

E.E. = 90 eV; v_m = 31V; σ = 18V

E.E. = 110 eV; v_m = 32V; σ = 18V

Apparently the higher electron energies produce more energetic ions which results in a slightly less Gaussian beam and increased beam spread. Of course, since the effective electron current and the total ionization cross section are dependent on

electron energy, the monotonic decrease of ion current with decreasing electron energy is expected.

It is also noted that for these results I.V. = +70V. Thus, positive ions are accelerated by an overall potential of 70V by the time they impinge on the ion collector plate. However, the results indicate that the voltage required to stop 50% of the extracted ions is about half this overall potential. Thus it is apparent that a large fraction of the extracted ions have not yet been fully accelerated by the point at which they pass through the retarding potential grid.

Argon.

Figure 7 presents total collected positive ion current versus source pressure for argon.. As for the nitrogen results, the behavior is reasonably linear with pressure. The indicated sensitivity is 1.2×10^{-4} A/torr. However, the pressures were determined directly from the ionization controller which was calibrated for nitrogen. Therefore, in order to determine a corresponding sensitivity for operation of the ion source with argon, the pressure reading should be corrected for the difference in the total ionization cross section. An estimate of this correction was obtained by using the ratio of the total ionization cross sections for nitrogen and argon at an electron energy of 110 eV from the data of Rapp and Englander-Golden (1965). In this manner, the resultant estimated sensitivity for argon increases to 1.3×10^{-4} A/torr.

The behavior of the total positive ion current versus filament current is presented in Figure 8. As shown, the behavior is quite similar to that obtained with nitrogen (*cf.* Figure 4). At the highest current of 2.9A, the "corrected" sensitivity for argon is 9.3×10^{-4} A/torr.

The behavior of the total collected positive ion current versus electron energy is presented in Figure 9. On the same graph are plotted total ionization cross sections for argon from Rapp and Englander-Golden (1965). As shown, the behavior is, once again, quite similar to that obtained for nitrogen (*cf.* Figure 5).

That is, while the total collected ion current does generally increase with electron energy, the qualitative behavior cannot be completely accounted for by the variation of the total ionization cross section alone.

Figure 10 presents total collected ion current versus retarding grid potential for argon. The results are quite similar to that obtained with nitrogen (*cf.* Figure 6), both qualitatively and quantitatively. Analysis of these data as previously assuming Gaussian beams yields the following "best fit" results:

$$\text{E.E.} = 70\ \text{eV};\ v_m = 25\text{V};\ \sigma = 18\text{V}$$

$$\text{E.E.} = 90\ \text{eV};\ v_m = 32\text{V};\ \sigma = 17\text{V}$$

$$\text{E.E.} = 110\ \text{eV};\ v_m = 33\text{V};\ \sigma = 20\text{V}$$

As for nitrogen, the beams apparently become more Gaussian at the lower electron energies.

Sulfur Hexafluoride.

The response of the total collected positive ion current with SF_6 pressure is presented in Figure 11. Although the behavior is reasonably linear over the range of pressures tested, the apparent sensitivity is 8.8×10^{-5} A/torr, which is less than for nitrogen and argon. However, the total ionization cross section for SF_6 is considerably greater than for either of these other two species (Rapp and Englander-Golden, 1965). An estimated correction of the ionization gauge pressures for this difference in cross sections is also presented in Figure 11. This correction increases the sensitivity to 2.3×10^{-4} A/.torr, which is more in line with that obtained for the other two gases.

The apparent differences in sensitivities for the various gases are not very great, and are almost completely due to differences in total ionization cross sections. In order to emphasize this point, all the current versus pressure data were reduced to a common nitrogen basis by first correcting the pressures as was done above, and

then correcting the collected currents by the ratio of total ionization cross sections according to the work of Rapp and Englander-Golden (1965). The results of these calculations are presented in Figure 12. As shown, all the data are almost collapsed to a common curve by this procedure, thereby substantiating the contention that ionization cross section differences, rather than other ion source extraction efficiencies are primarily responsible for the varying sensitivities observed.

The behavior of the total collected positive ion current versus electron energy is presented in Figure 13 for sulfur hexafluoride. As previously, on the same graph are plotted total ionization cross sections for SF_6 from Rapp and Englander-Golden (1965). The behavior is qualitatively similar to that observed for nitrogen (*cf.* Figure 5) and argon (*cf.* Figure 9). However, in the case of the SF_6 data, the monotonic increase in collected current with electron energy appears to follow the increase in total ionization cross section more closely than for the other two gases. This may be because the increase in total ionization cross section over the electron energy range investigated is greater than that for the other two gases, and, consequently, is the controlling characteristic.

Figure 14 presents total collected ion current versus retarding grid potential for sulfur hexafluoride. The results are quite similar to that obtained with nitrogen (*cf.* Figure 6), both qualitatively and quantitatively. Analysis of these data as previously assuming Gaussian beams yields the following "best fit" results:

$$\text{E.E.} = 70\ \text{eV};\ v_m = 25\text{V};\ \sigma = 17\text{V}$$

$$\text{E.E.} = 90\ \text{eV};\ v_m = 32\text{V};\ \sigma = 17\text{V}$$

$$\text{E.E.} = 110\ \text{eV};\ v_m = 38\text{V};\ \sigma = 17\text{V}$$

As for nitrogen, the beams appear to become more Gaussian at the lower electron energies.

Source Magnets.

The effect of permanent magnets on the performance of the prototype ion source was investigated in a series of tests. Two ALNICO magnets (~1 Gauss) were mounted on the source in the positions shown in the schematics, Figure 1(a) and 2(a). The two bar magnets were mounted such that their magnetic field lines were approximately collinear with the electron beam sheet. In this manner, any velocity component of the electrons perpendicular to the magnetic field lines would induce cyclotronic motion which, when coupled to the directed velocity towards the electron collector, would produce a helical path through the ion volume. This would tend to increase the ionization efficiency of the electron beam primarily by increasing the effective pathlength through the ion volume.

The particular magnets tested were not very effective in this role. As shown in Figure 15, in all cases, for all the gases tested, use of the magnets either had no discernible effect, or actually decreased the ion source performance slightly in terms of total collected ion current. However, use of the magnets did have the beneficial effect of essentially eliminating the background current at the ion collector due to stray electrons. Thus was interpreted to mean that the magnets probably did improve the retention of emitted electrons within the ion volume, but that the extraction efficiency of the ions could not be increased sufficiently to capitalize on this effect. If this is indeed the case, then magnets with a greater field strength should improve the performance of the ion source.

Although the elimination of the background current at the ion collector was found to be quite useful in the current test mode, it might not prove as useful in combination with a mass spectrometer since the "onblast" signal at m/e = 0 can be easily eliminated *via* resolution adjustments of the quadrupole rod control circuitry.

2.3. Negative Ion Source.

2.3-1. Background.

Negative ions are generally more difficult to produce than positive ions due to their different mechanisms of formation. For example, the ionization of methane with 90 eV electrons produces an intensity ratio of the two most abundant positive and negative ions of $CH_4^+/C^- \sim 10^4$. Thus, apparently negative ion formation in this case exhibits a significantly lower cross section than positive ion formation. In addition, negative ions are often formed with excess kinetic energy, which reduces their collection efficiency in a mass spectrometer.

For electron energies greater than about 3--40 eV, the relative abundances of positive ions produced are generally independent of energy, and, indeed positive ion mass spectra of many compounds have been determined under such conditions. Negative ion abundances, on the other hand, cannot be similarly tabulated because of their different modes of formation. At energies ~<2 eV they are formed primarily by electron capture; at 2-10 eV by dissociative resonance capture; and at ~70 eV by ion-pair formation (e.g., see McDaniel, 1964; Price and Williams, 1969). Consequently, the ions observed and their relative abundances are markedly dependent on electron energy. In addition, at high source pressures, all three formation modes may take place simultaneously due to secondary reactions, and ion abundances may exhibit different pressure dependencies.

One of the major differences between positive and negative ion formation lies in the narrow resonance peak dependence of the cross section for negative ion formation on electron energy in the resonance capture regime. Dissociative attachment cross sections for some negative ions are presented in Table 2 (Rapp and Briglia, 1965). As shown, for most gases the total cross sections for the production of negative ions by dissociative resonance capture are orders of magnitude less than

that for the formation of positive ions. The only exception in the table is SF_6. Moreover, the resonance nature of the capture process makes the cross sections peak sharply at relatively low electron energies. Thus low electron energies are necessary for negative ion formation *via* resonance dissociative electron capture. However, at *ca.* 70 eV and source pressures of ~10^{-5} torr, the ion-pair formation mechanism dominates. Under these conditions many halogenated compounds form negative ions.

2.3-2. Results and Discussion.

In view of the success of the prototype design as a positive ion source, it was decided to apply the same basic design to the production of negative ions. SF_6 was used as the test gas.

In order for the electron impact ion source to be used as a negative ion source, the sense of some of the biases must be reversed. In order to collect the negative ions on the collector plate, the ion volume must be negatively biased with respect to the vacuum system ground. The extraction potential (X) must be positive with respect to the ion volume. The electron collector must remain positive with respect to the ion volume; however, the energetic fragment ions formed by dissociative ionization must be prevented from being collected on the positively biased electron collector. This is usually accomplished by increasing the bias on the extraction electrode. Unfortunately, however, this strategy can lead to electrons also being extracted from the ion source at high extraction voltages. Thus, a more careful balancing of potentials must be achieved in the negative ion mode than in the positive ion mode. Consistent results could not be obtained without the magnets in place. This was attributed primarily to excessive penetration of the electrons from the ion source volume to the ion collector plate, such that the relatively smaller

negative ion fraction could not be differentiated. However, consistent results were obtained in the negative ion mode with SF_6 as the test gas when the source magnets were used. Apparently, the magnets effectively decreased the stray electron current sufficiently to allow use of the retarding potential grid to eliminate the residual electron current which escaped from the ion volume. Because of this problem, the negative ion current was quite sensitive to the retarding grid potential, and therefore, ion energy effects could not be investigated as for the positive ion source.

The biasing configuration which was found to yield the best performance was: I.V. = -15V; E.E. ~ 1 eV; X = 40V; F = 20V; R = -60V; C = +35V. The data presented in Figure 16 were obtained under these conditions. As can be seen, there are some significant differences between the behavior of the ion source in the negative ion mode versus the positive ion mode. First of all, the collected ion currents are about two orders of magnitude less than for comparable conditions in the positive ion mode. Although this is considerably less than the factor of three or so suggested by the data in Table 2 for SF_6, the lowest electron energy that could be reliably obtained with the prototype configuration was on the order of 1 eV, rather than 0.1 eV, as indicated in Table 2. Thus the efficiency of negative ion production was probably less.

As shown in Figure 16, although the behavior with pressure is monotonic, it is not very linear. Also, the "best fit" lines do not pass through the origin as they do in the positive ion mode. This can be due to several factors, but most likely it is the result of a small residual electron current which could not be completely eliminated by the retarding grid. In any case, the linear fits yield an "apparent" sensitivity of 7.5×10^{-7} A/torr, and a "corrected" (for ionization gauge tube performance) of 2×10^{-6} A/torr.

The behavior of the ion current with filament current was also decidedly different than found for the positive ion source. Typical data are presented in Figure

17. As shown, a monotonic increase in negative ion current with filament current was not obtained. This is ascribed to the much more sensitive biasing, focusing, and extraction problems encountered for operation in the negative ion mode.

In summary, it is concluded that the current prototype design is capable of producing negative ion beams, but that more work is needed to optimize the conditions for performance.

3.0. Summary and Conclusions.

Prototype ion sources were developed, constructed, and tested for operation in both positive and negative ion modes. In the positive ion mode, sensitivities of almost 10^{-3} A/torr can be obtained at the highest filament currents tested. Even under less stringent filament operating conditions, sensitivities typically exceed 10^{-4} A/torr. This range of sensitivities is quite comparable to that reported by manufacturers for ion sources used on commercial mass spectrometers: e.g., Ametek-Dycor, 2.8 x 10^{-4} A/torr @ 2 mA emission, 2 x 10^{-4} A/torr @ 1 mA emission; Granville-Phillips Spectrascan 750 (Finnigan), 10^{-3} A/torr @ 2 mA emission; UTi 100C, 1.8 x 10^{-3} A/torr @ 2.7 mA emission.

Total collected ion currents in the positive ion mode were reasonably linear over about an order of magnitude in pressure. The collected ion current generally increases with electron energy, following somewhat, but not completely, the trend with total ionization cross section. Therefore, various extraction and focusing efficiencies figure strongly in the ion intensities that are actually obtained.

The results of energy analysis of the ion beams are consistent with Gaussian beams with relatively wide variances. Typical beam energies peaked in the regime of 30-35V, with variances of 17-18V. The ion beams did not appear to be fully accelerated at the analyzing electrode. The beams generally seem to become more

Gaussian with reduced variances at the lower electron energies.

The use of magnets did not improve ion source performance in the positive ion mode in terms of total collected ion current. However, it did eliminate a significant background current problem at the collector plate.

In the negative ion mode, total collected negative ion currents using SF_6 were approximately two orders of magnitude less than under comparable conditions in the positive ion mode. Use of the source magnets was essential to obtaining data in this case. Although the ion source did produce negative ion beams, the source design could still be improved upon.

REFERENCES

Hunton, D.E., and Calo, J.M., "Low energy ions in the Shuttle environment: Evidence for strong ambient-contaminant interactions," *Planet. Space Sci.* **33,** 945 (1985).

Hunton, D.E., Viggiano, A.A., Swider, W., Paulson, J.F., and Sherman, C., "Mass spectrometric measurements of SF_6 chemical releases from sounding rockets," *J. Geophys. Res.* **92,** 8827 (1987).

Knewstubb, P.F. *Mass Spectrometry and Ion-Molecule Reactions,* Cambridge University Press, 1969.

McDaniel, E.W. *Collision Phenomena in Ionized Gases,* Wiley & Sons, NY, 1964, p. 382.

Mende, S.B., Garriott, O.K., and Banks, P.M., "Observations of optical emissions on STS-4," *Geophys. Res. Lett.* **10,** 122 (1983).

Narcisi, R.S., and Roth, W. "The formation of cluster ions in laboratory sources and in the ionosphere," in Adv. Electr. and Electr. Phys., Academic Press, NY, Vol. 29, 1970, p. 79.

Narcisi, R.S., Bailey, A.D., Della Lucca, L., Sherman, C., and Thomas, D.M. Mass spectrometric measurements of negative ions in the D- and lower E-regions, *J. Atm. Terr. Phys.* **33,** 1147-1159, 1971.

Price, D., and Williams, J.E. *Time-of-Flight Mass Spectrometry,*Pergamon Press, London, 1969.

Rapp, D., and D.D. Briglia, "Total cross sections for ionization and attachment in gases by electron impact. II. Negative ion formation," *J. Chem. Phys.* **43,** 1480 - 1489 (1965).

Rapp, D., and Englander-Golden, "Total cross sections for ionization and attachment in gases by electron impact. I. Positive ionization," *J. Chem. Phys.* **43,** 1464 - 1479 (1965).

Table 1. Ion source elements and applied potentials.

Designation	Description
G	ground (vacuum system)
I.C.	ion collector plate
E.E.	electron energy
I.V.	ion volume potential w.r.t G
C	electron collector potential w.r.t. I.V.
F	focus plate potential w.r.t. I.V.
X	extractor plate potential w.r.t. I.V.
R	retarding potential grid w.r.t. I.V.

Table 2. Dissociative electron capture and total ionization cross sections for various gases (Rapp and Briglia, 1965).

Gas	E_T (eV)	E_A (eV)	$\sigma_A(E_A)/\sigma_T(E_T)$	$\sigma_A(E_A)$
O_2	118	6.5	5.16×10^{-2}	0.0160
CO	99	9.9	7.64×10^{-4}	0.00230
NO	118.5	8.15	3.5×10^{-3}	0.0127
CO_2	118	8.1	1.205×10^{-3}	0.00487
N_2O	109	2.2	2.29×10^{-2}	0.0978
SF_6	110	~0.1	0.32	2.44
H_2	69	13.9	2.01×10^{-4}	2.22×10^{-4}

E_A = electron energy at resonance capture maximum.

E_T = electron energy at which the total ionization cross section was measured.

$\sigma_A(E_A)$ = cross section for negative ion formation by dissociative resonance (in units of ion cross section, πa_o^2)

$\sigma_T(E_T)$ = total ionization cross section

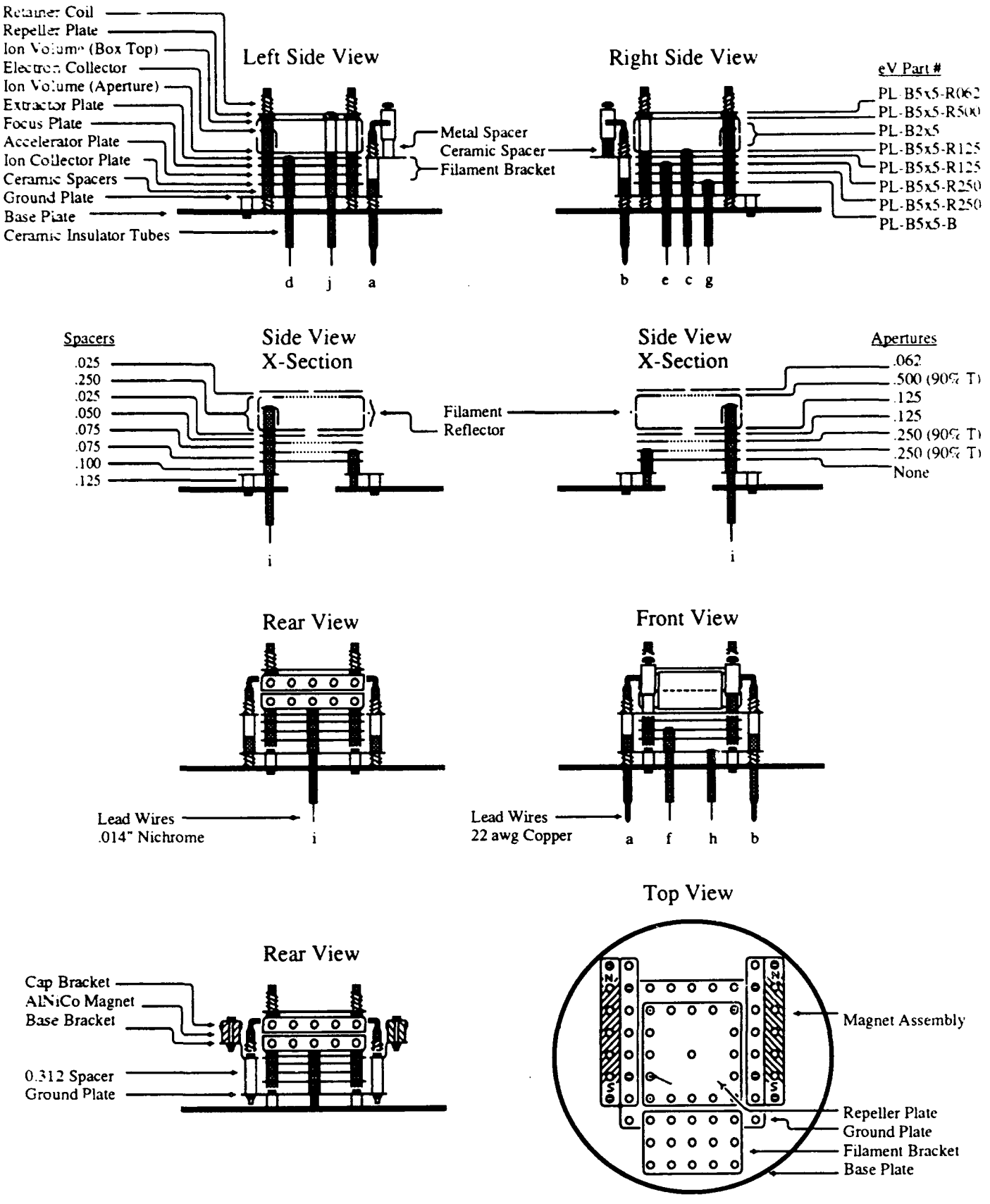

Figure 1(a). Schematic of ion source #1.

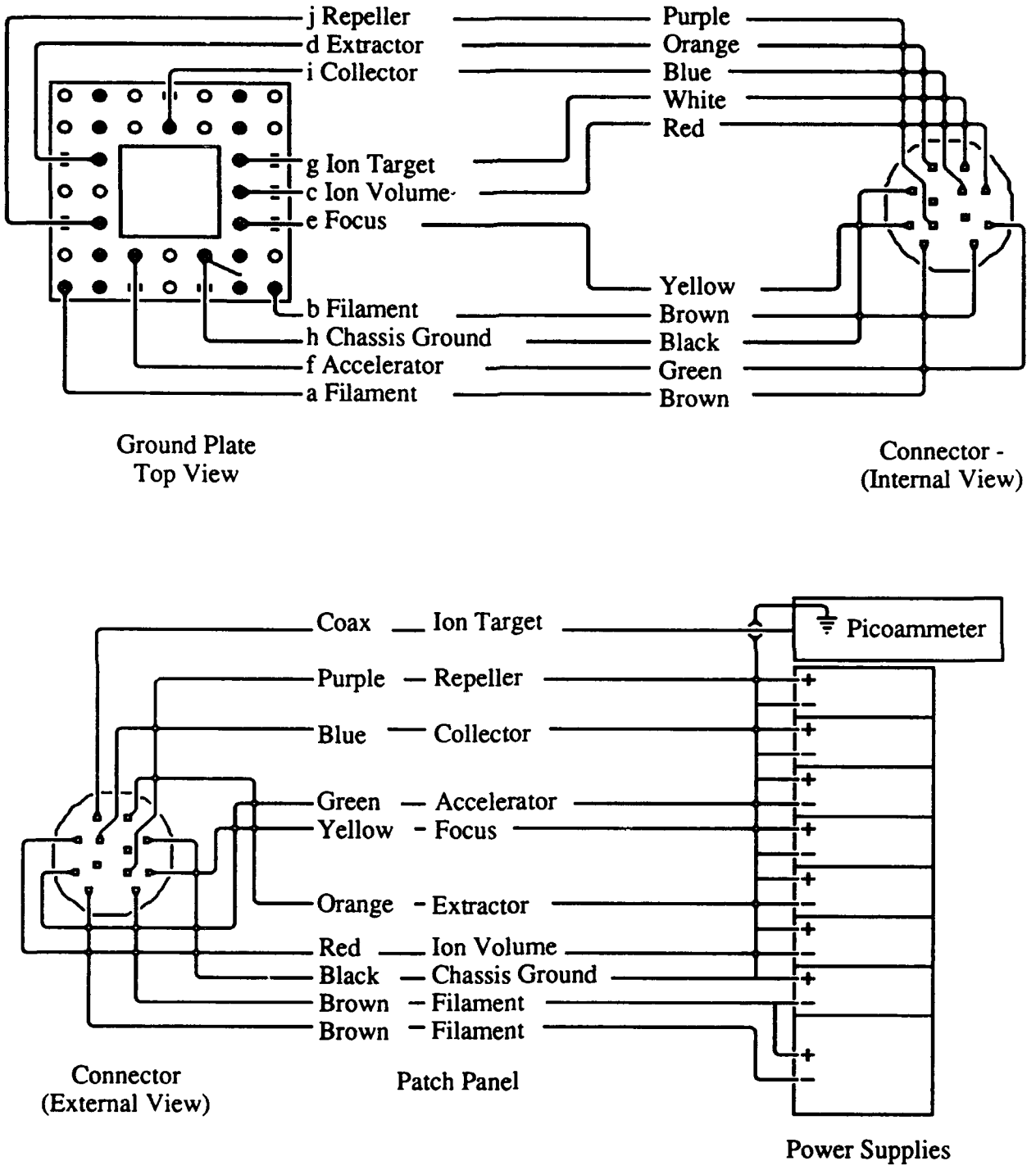

Figure 1(b). Wiring diagram for ion source #1.

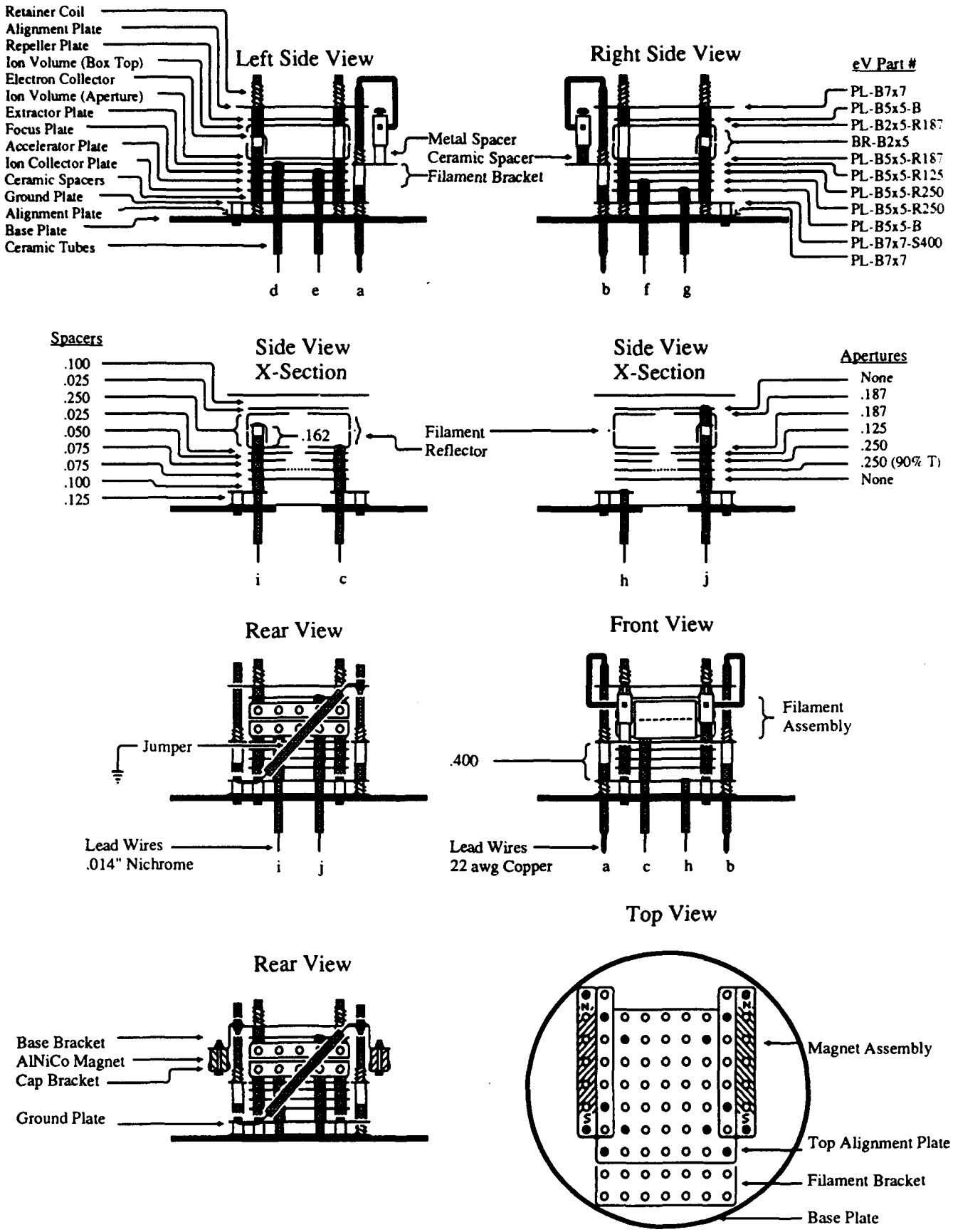

Figure 2(a). Schematic of ion source #2.

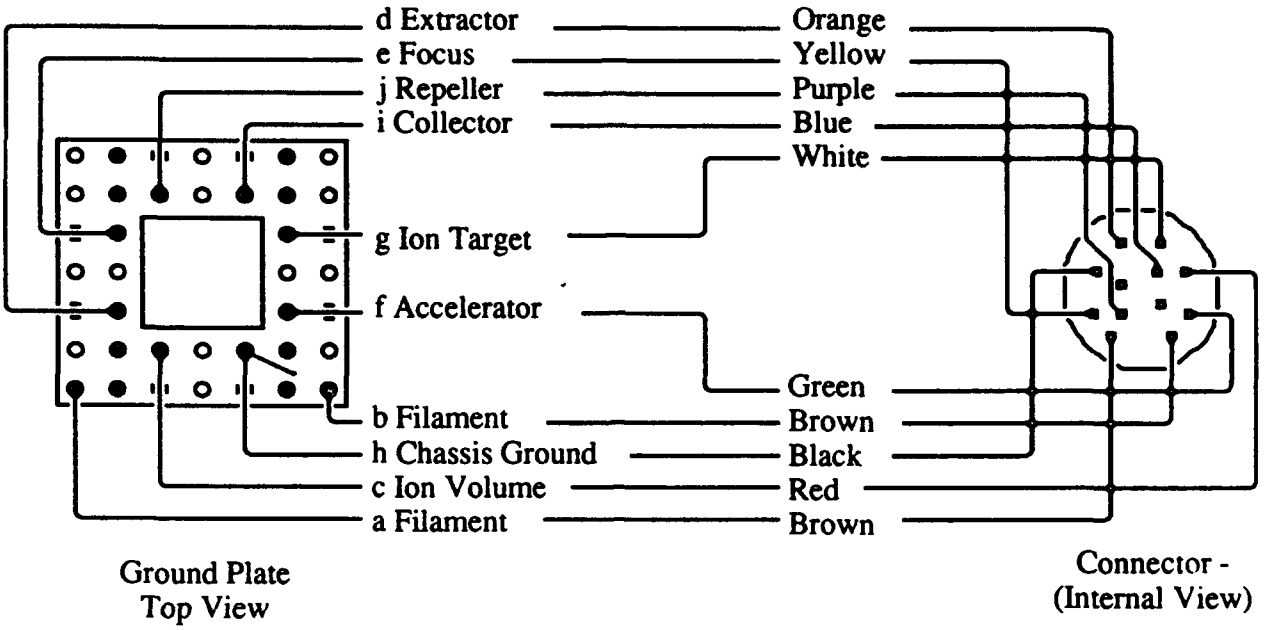

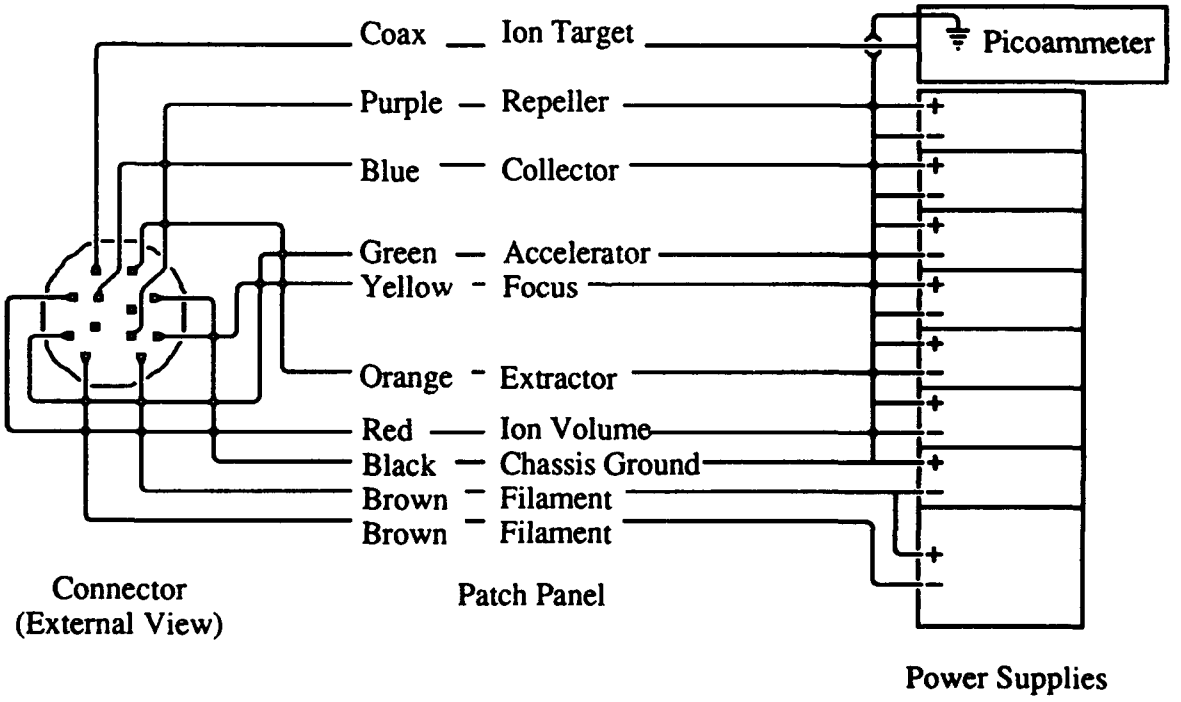

Figure 2(b). Wiring diagram for ion source #2.

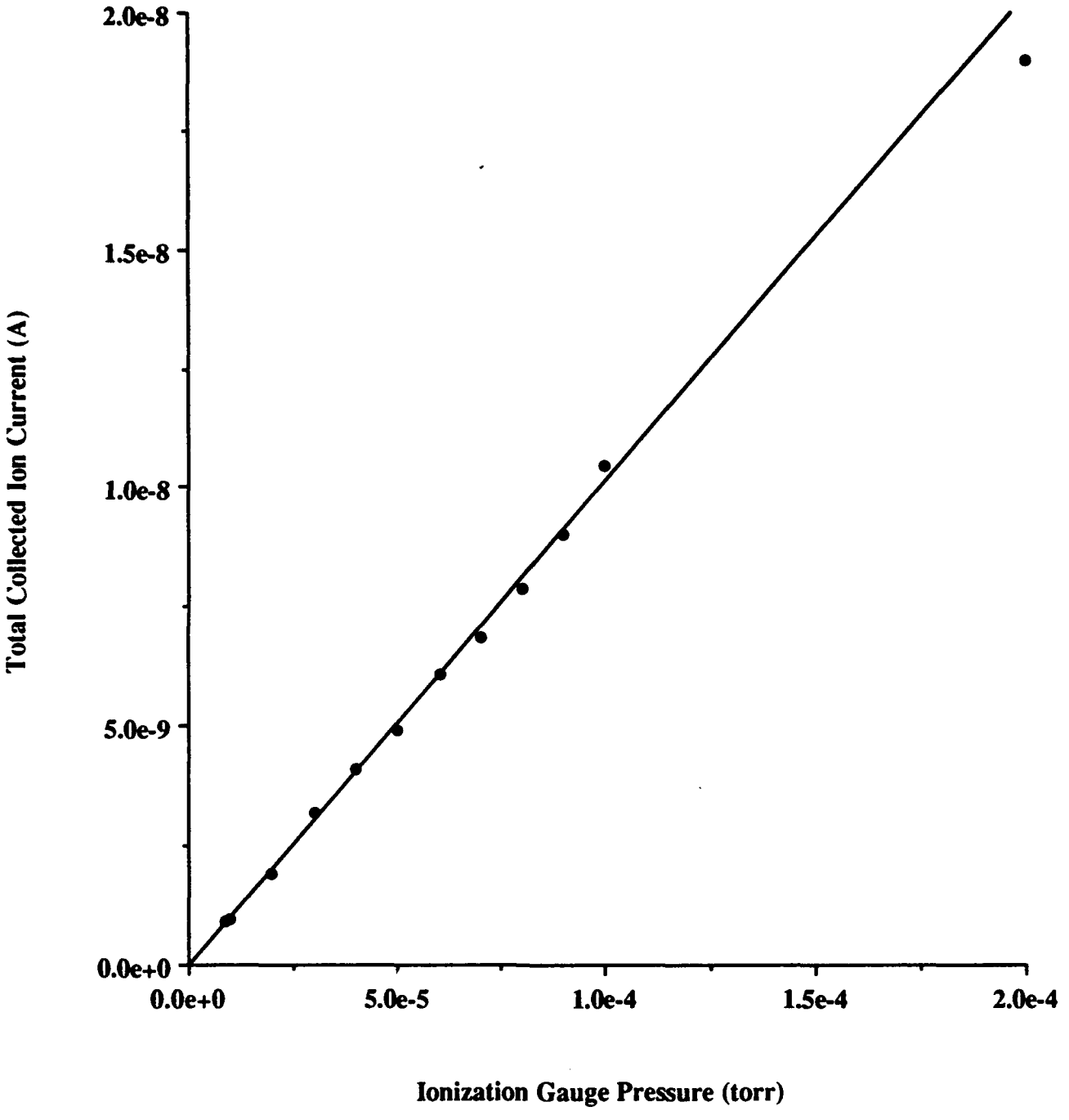

Figure 3. Total positive ion current as a function of pressure for nitrogen. Sensitivity: 1.1 x 10^{-4} A/torr. Ion source configuration: E.E. = 110 eV; I.V. = 70V; X = -20V; F = -20V; R = -25V; C = +35V.

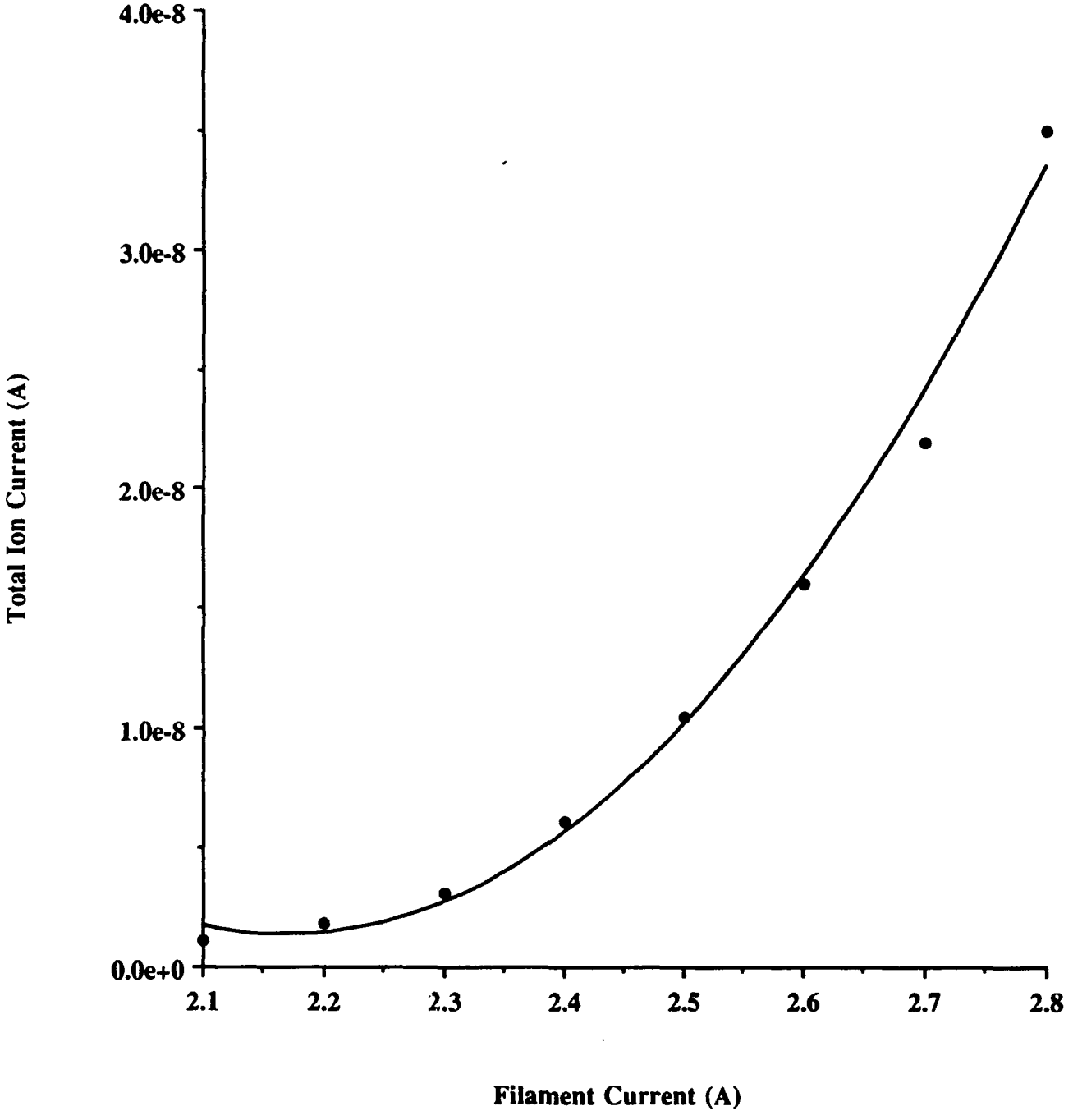

Figure 4. Total positive ion current as a function of filament current for nitrogen at a pressure of 1 x 10^{-4} torr. Ion source configuration: E.E. = 110ev; X = -20V; F = -20V; R = -25V; C = +35V.

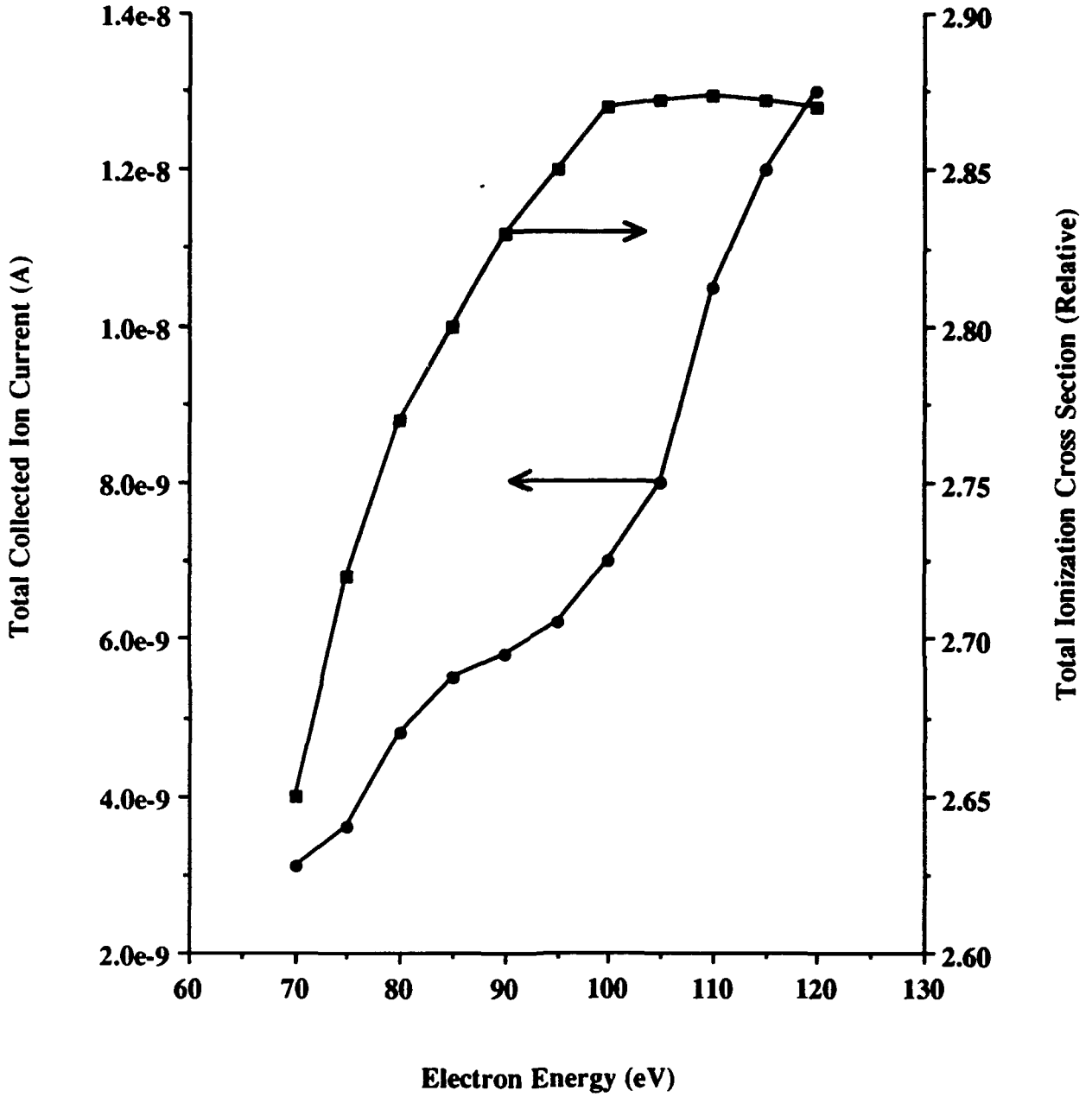

Figure 5. Total positive ion current and total ionization cross sections (Rapp and Englander-Golden, 1965) as a function of electron energy for nitrogen at 1 x 10^{-4} torr. Ion source configuration: I.V. = 70V; X = -20V; F = -20V; R = -25V; C = +35V.

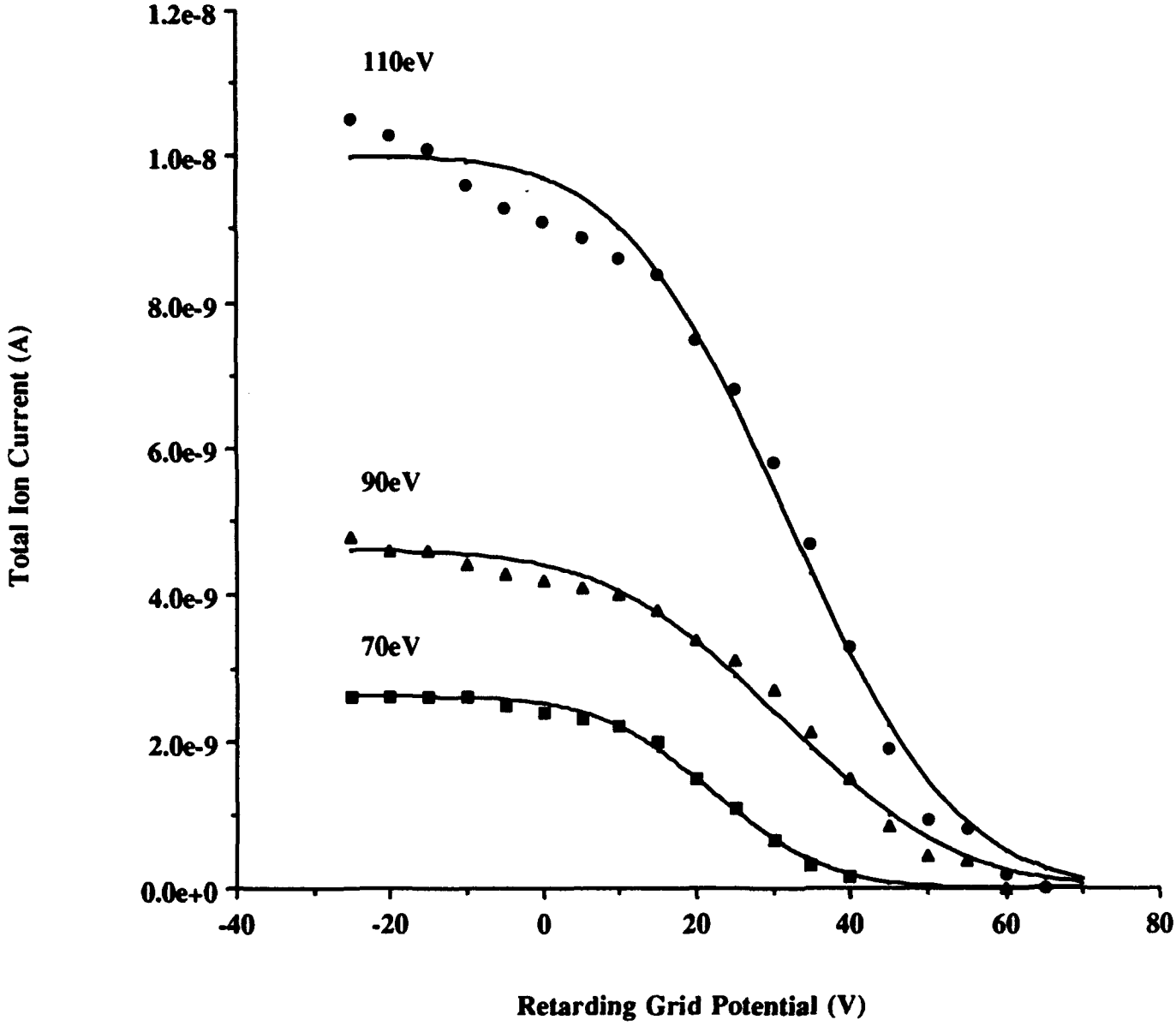

Figure 6. Total positive ion current as a function of retarding grid potential for three values of the electron energy for nitrogen at 1 x 10^{-4} torr. Ion source configuration: X = -20V; F = -20V; C = +35V. The solid curves are the "best fits" obtained assuming Gaussian beams. The resultant means and variances of the beams are: 70 eV, v_m = 22V, σ = 12V; 90 eV, v_m = 31V, σ = 18V; 110 eV, v_m = 32V, σ = 18V.

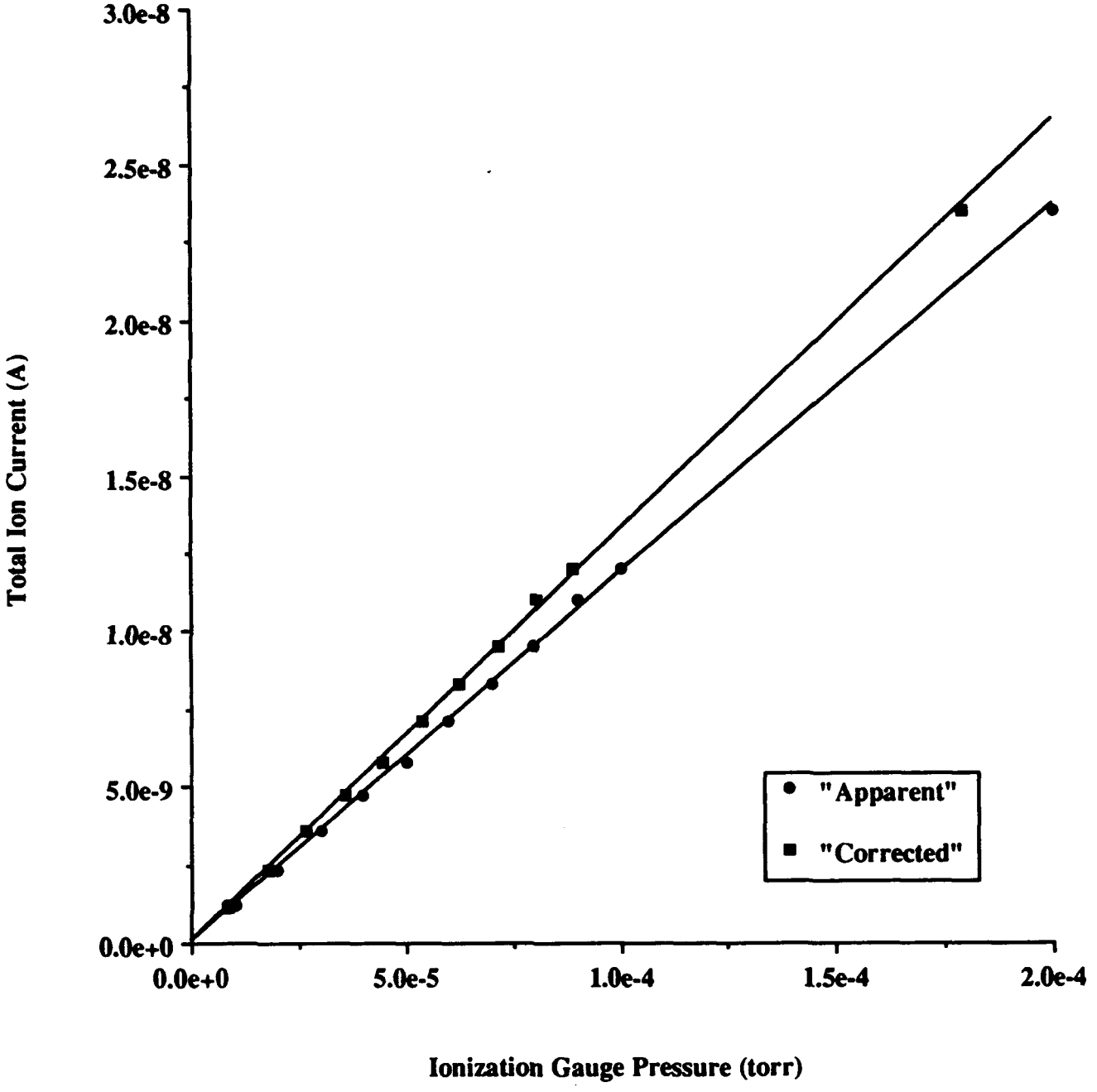

Figure 7. Total positive ion current as a function of pressure for argon. "Apparent" and "corrected" sensitivities are 1.2 x 10^{-4} and 1.3 x 10^{-4} A/torr, respectively. Ion source configuration: E.E. = 90 eV; I.V. = 70V; X = -20V; F = -20V; R = -25V; C = +35V.

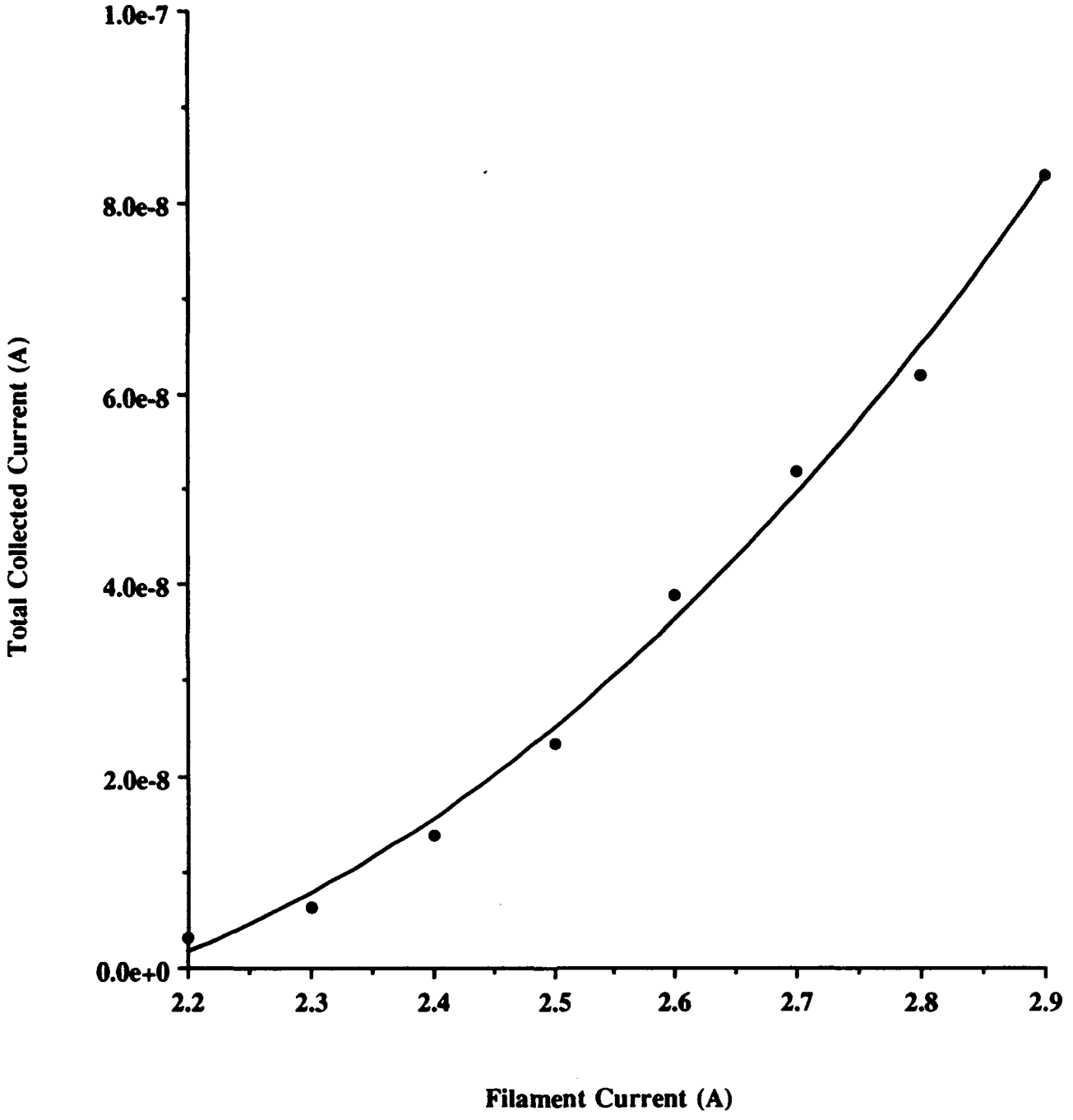

Figure 8. Total positive ion current as a function of filament current for argon at an ionization gauge pressure of 2 x 10^{-4} torr. Ion source configuration: E.E. = -90ev; X = -20V; F = -20V; R = -25V; C = +35V.

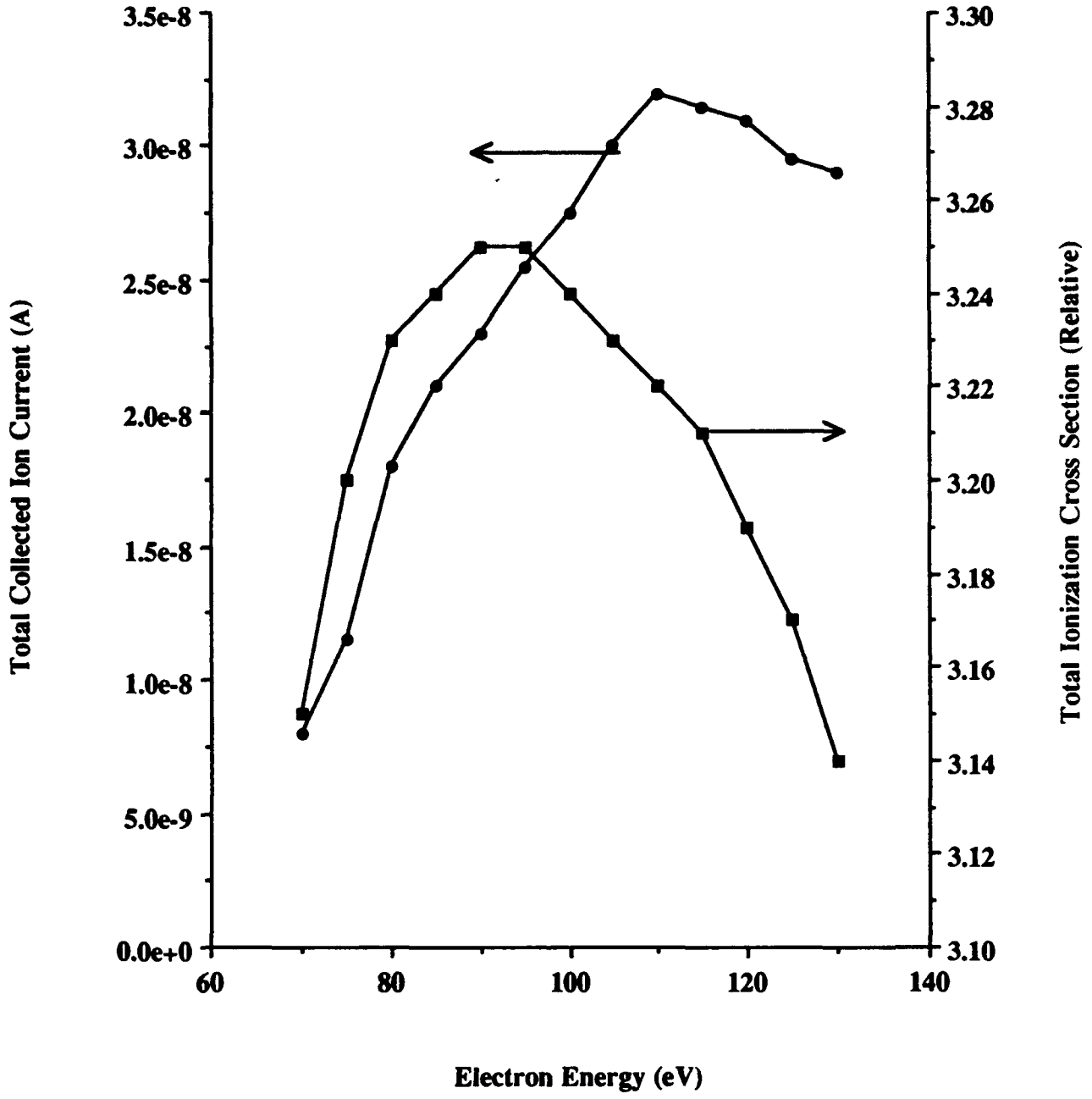

Figure 9. Total positive ion current and total ionization cross sections (Rapp and Englander-Golden, 1965) as a function of electron energy for argon at an ionization gauge pressure of 2 x 10^{-4} torr. Ion source configuration: I.V. = 70V; X = -20V; F = -20V; R = -25V; C = +35V.

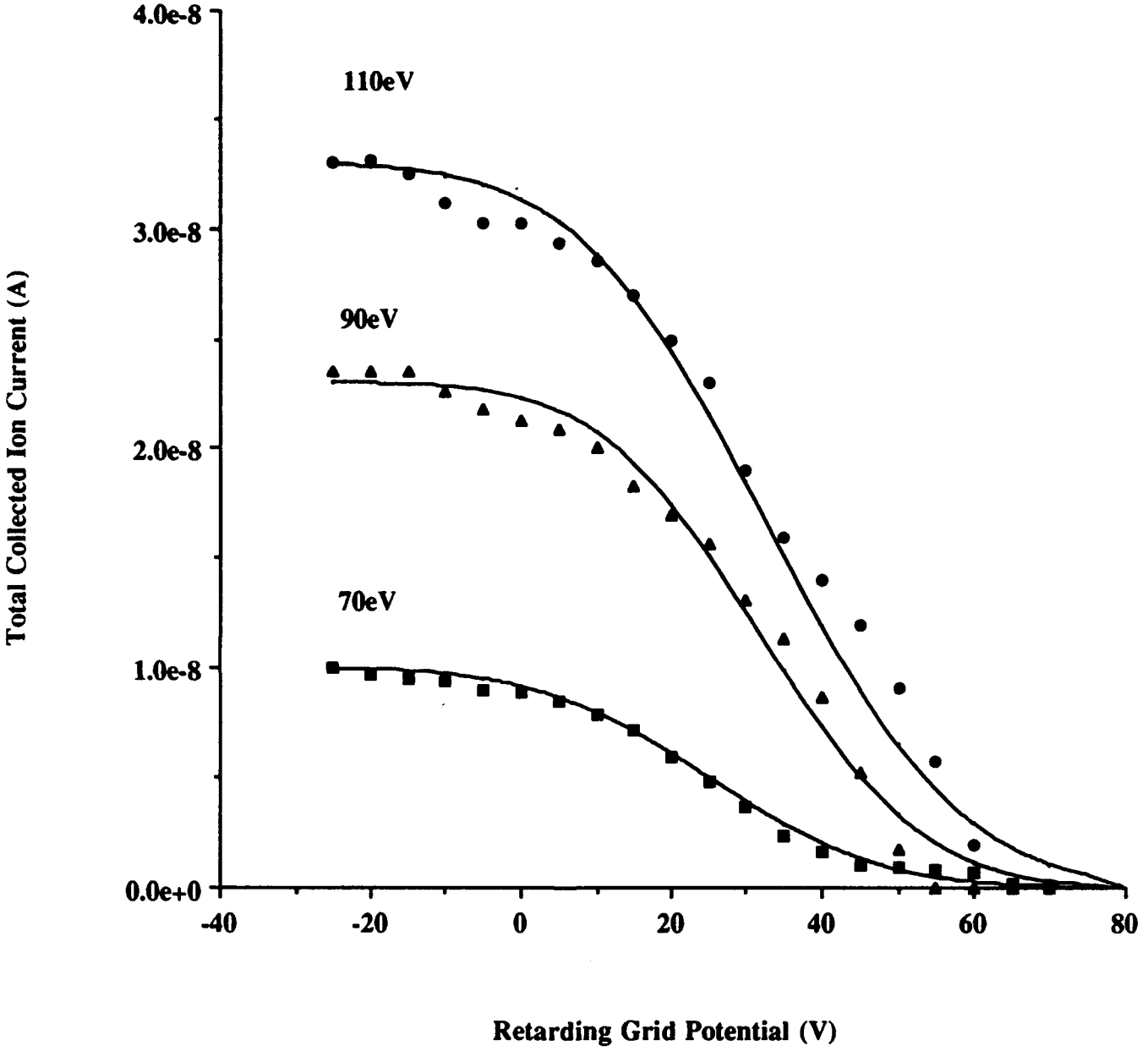

Figure 10. Total positive ion current as a function of retarding grid potential for three values of the electron energy for argon at an ionization gauge pressure of 2 x 10^{-4} torr. Ion source configuration: X = -20V; F = -20V; C = +35V. The solid curves are the "best fits" obtained assuming Gaussian beams. The resultant means and variances of the beams are: 70 eV, v_m = 25V, σ = 18V; 90 eV, v_m = 32V, σ = 17V; 110 eV, v_m = 33V, σ = 20V.

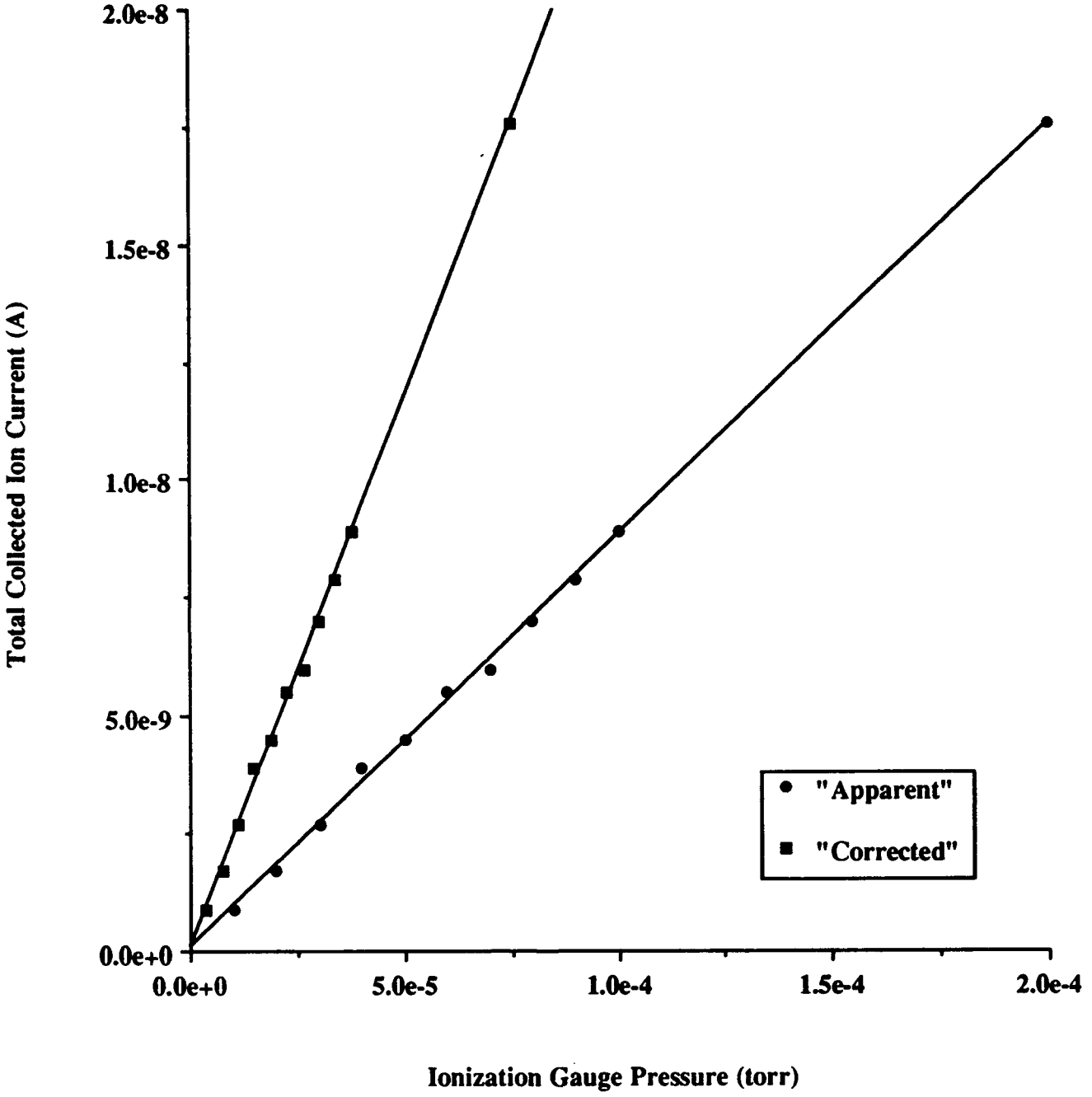

Figure 11. Total positive ion current as a function of pressure for sulfur hexafluoride. "Apparent" and "corrected" sensitivities are 8.8 x 10^{-5} and 2.3 x 10^{-4} A/torr, respectively. Ion source configuration: E.E. = 90 eV; I.V. = 70V; X = -20V; F = -20V; R = -25V; C = +35V.

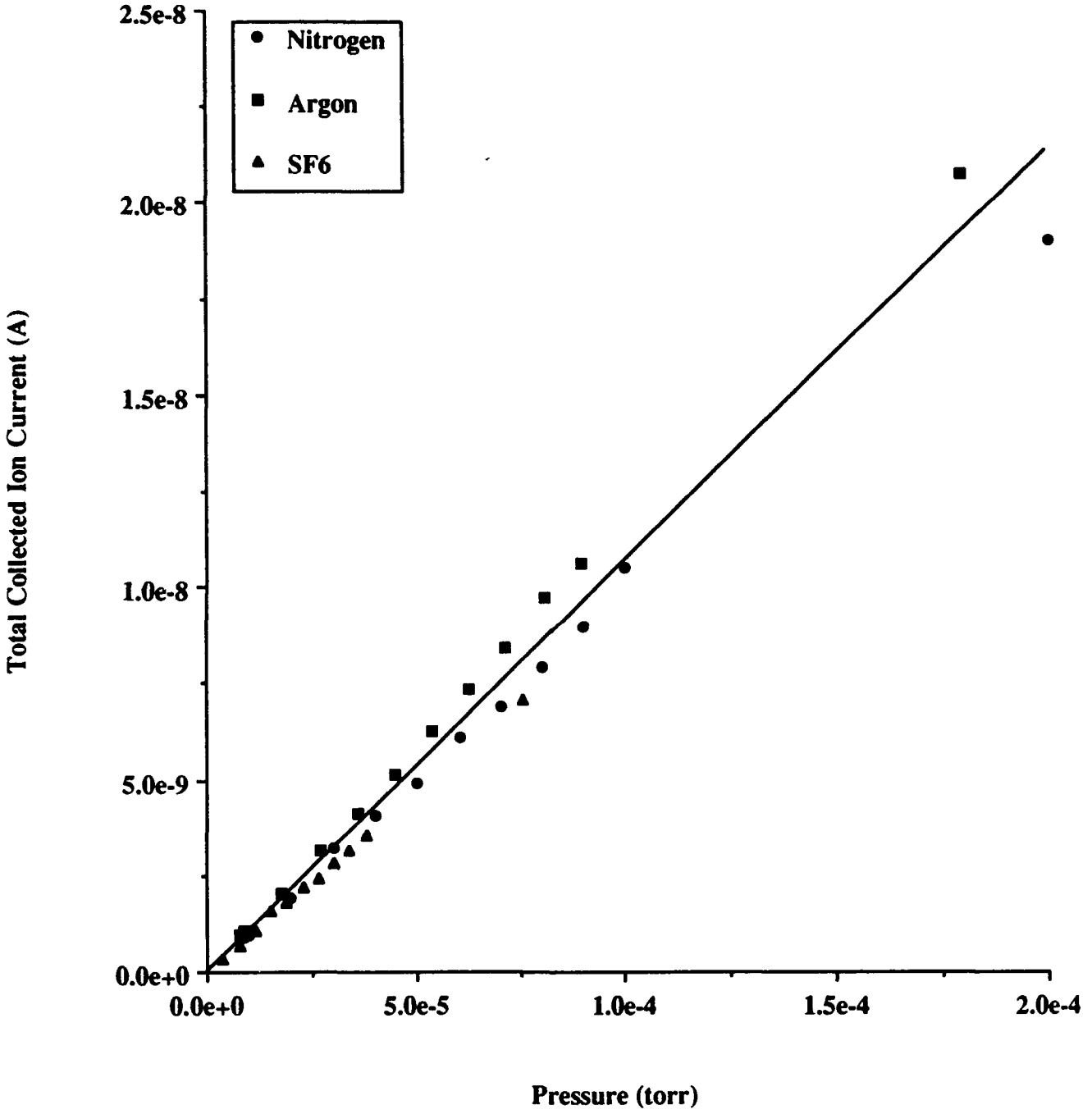

Figure 12. Total positive ion current as a function of pressure for the three gases tested, corrected to a common (nitrogen) basis. Ion source configuration: E.E. = 90 eV; I.V. = 70V; X = -20V; F = -20V; R = -25V; C = +35V.

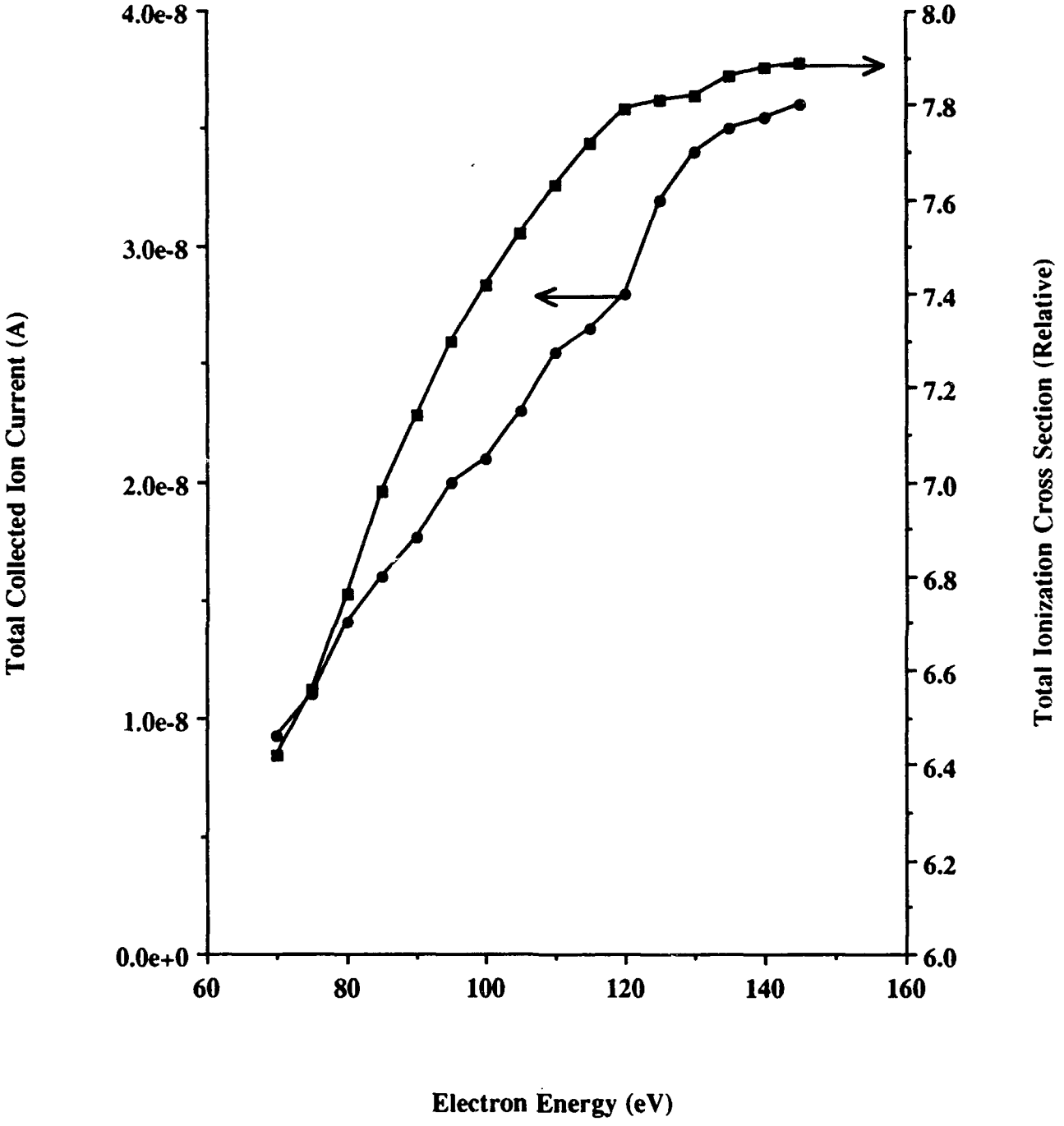

Figure 13. Total positive ion current and total ionization cross sections (Rapp and Englander-Golden, 1965) as a function of electron energy for sulfur hexafluoride at an ionization gauge pressure of 2 x 10^{-4} torr. Ion source configuration: I.V. = 70V; X = -20V; F = -20V; R = -25V; C = +35V.

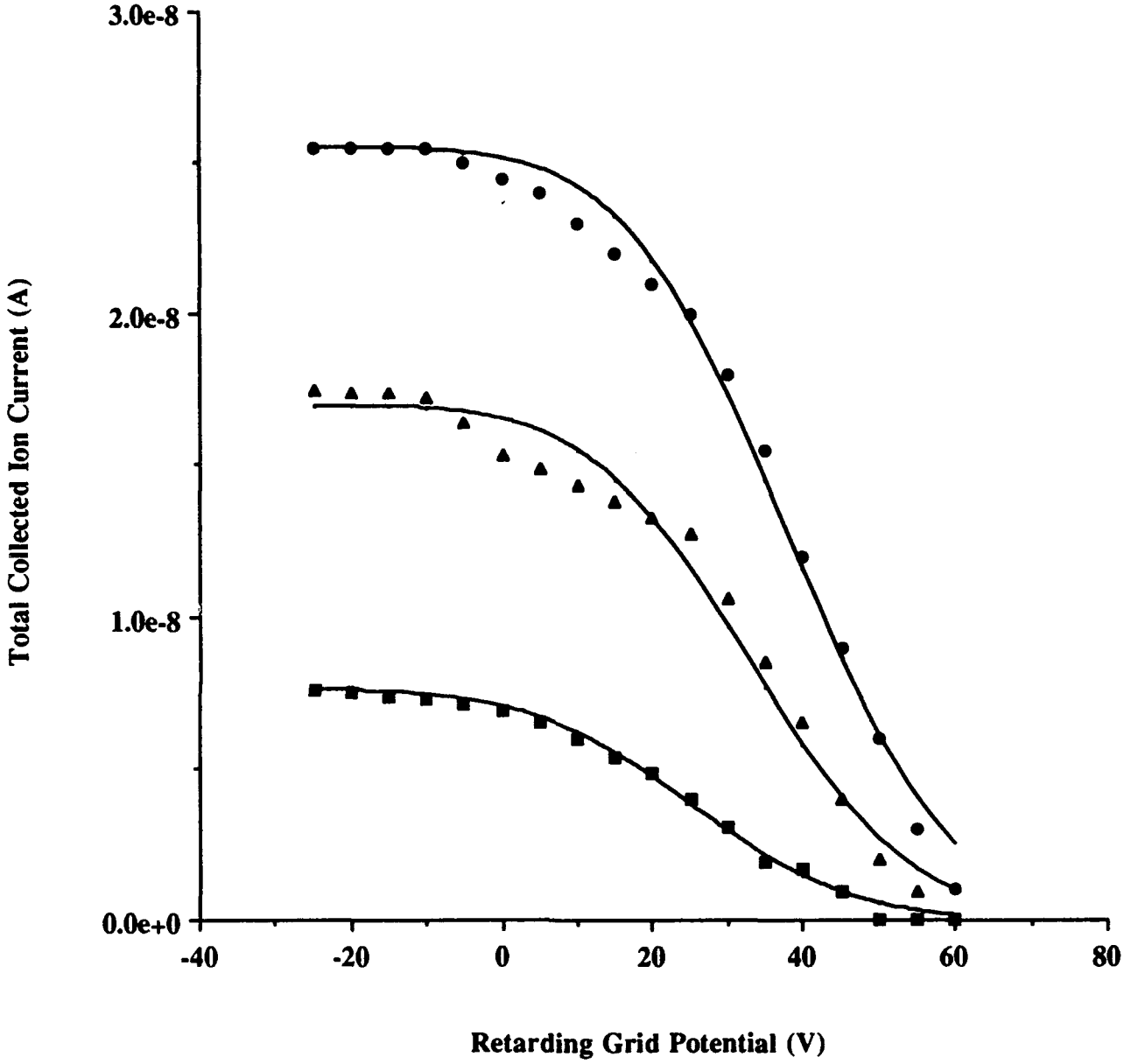

Figure 14. Total positive ion current as a function of retarding grid potential for three values of the electron energy for sulfur hexafluoride at an ionization gauge pressure of 2 x 10^{-4} torr. Ion source configuration: X = -20V; F = -20V; C = +35V. The solid curves are the "best fits" obtained assuming Gaussian beams. The resultant means and variances of the beams are: 70 eV, v_m = 25V, σ = 17V; 90 eV, v_m = 32V, σ = 17V; 110 eV, v_m = 38V, σ = 17V.

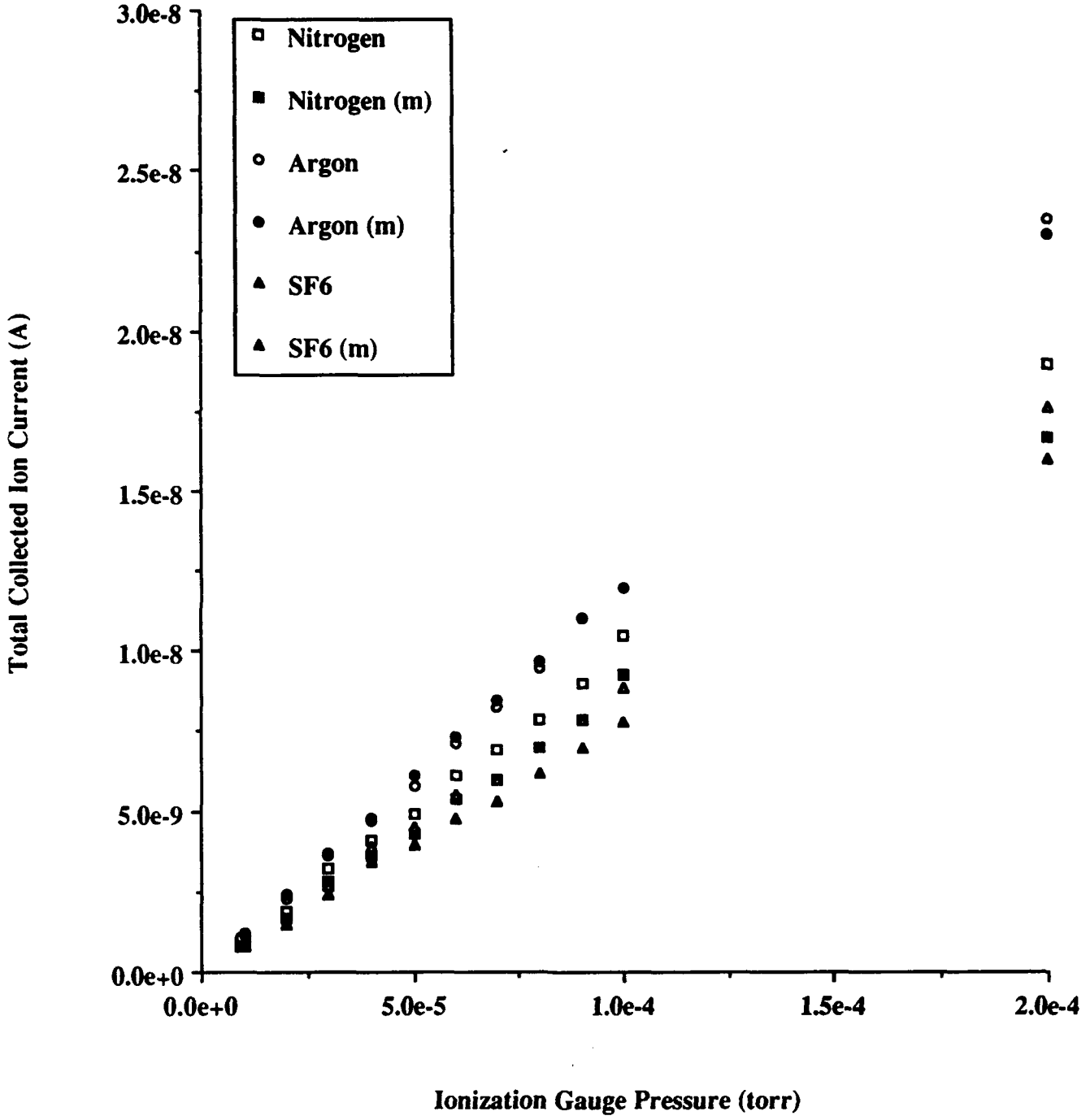

Figure 15. Total positive ion current as a function of ionization gauge pressure for the ion source operated both with and without magnets, for the three gases tested.

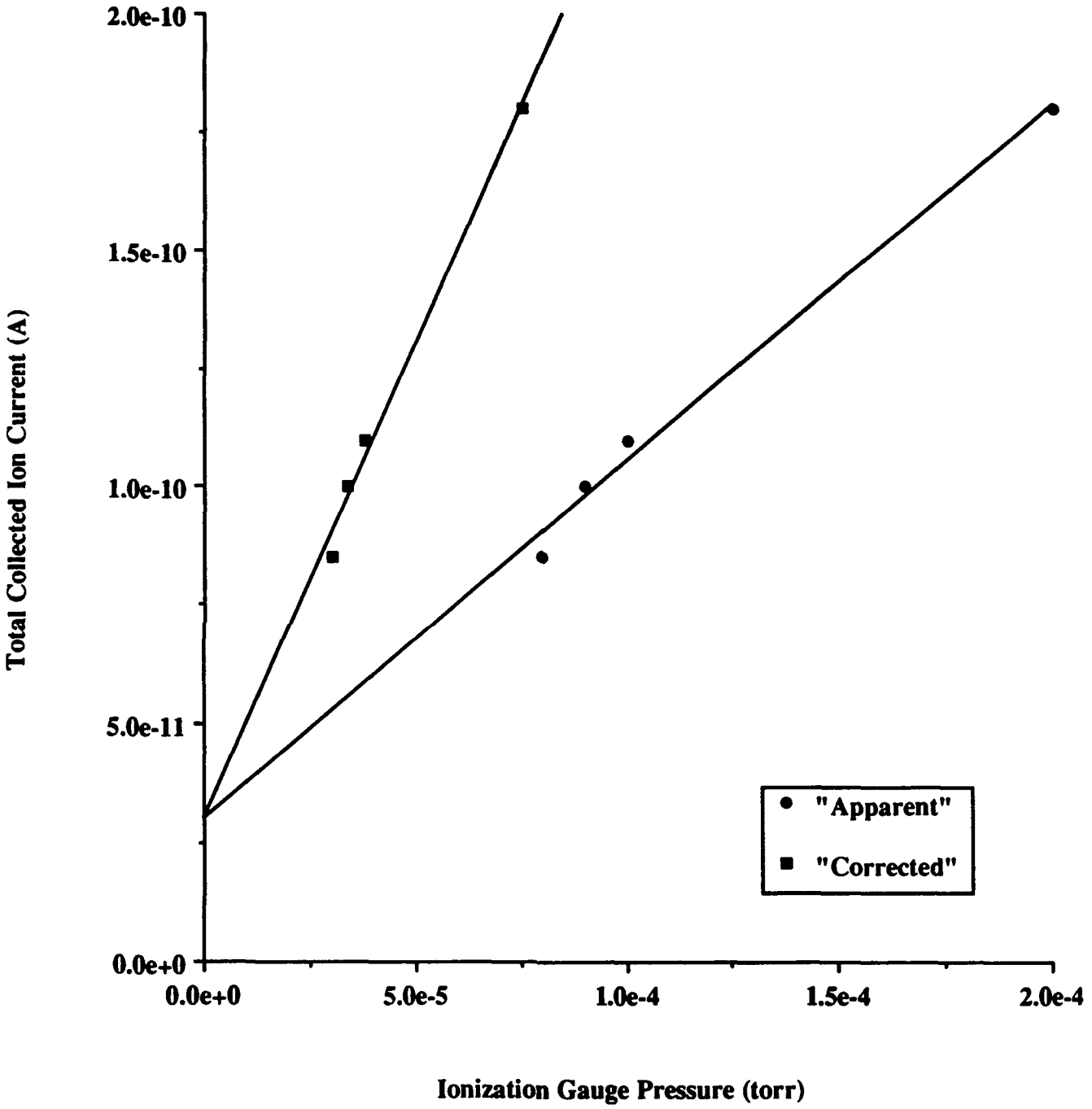

Figure 16. Total negative ion current as a function of ionization gauge pressure for sulfur hexafluoride. Ion source configuration: I.V. = -15V; E.E. ~ 1 eV; X = 40V; F = 20V; R = -60V; C = +35V; with magnets.

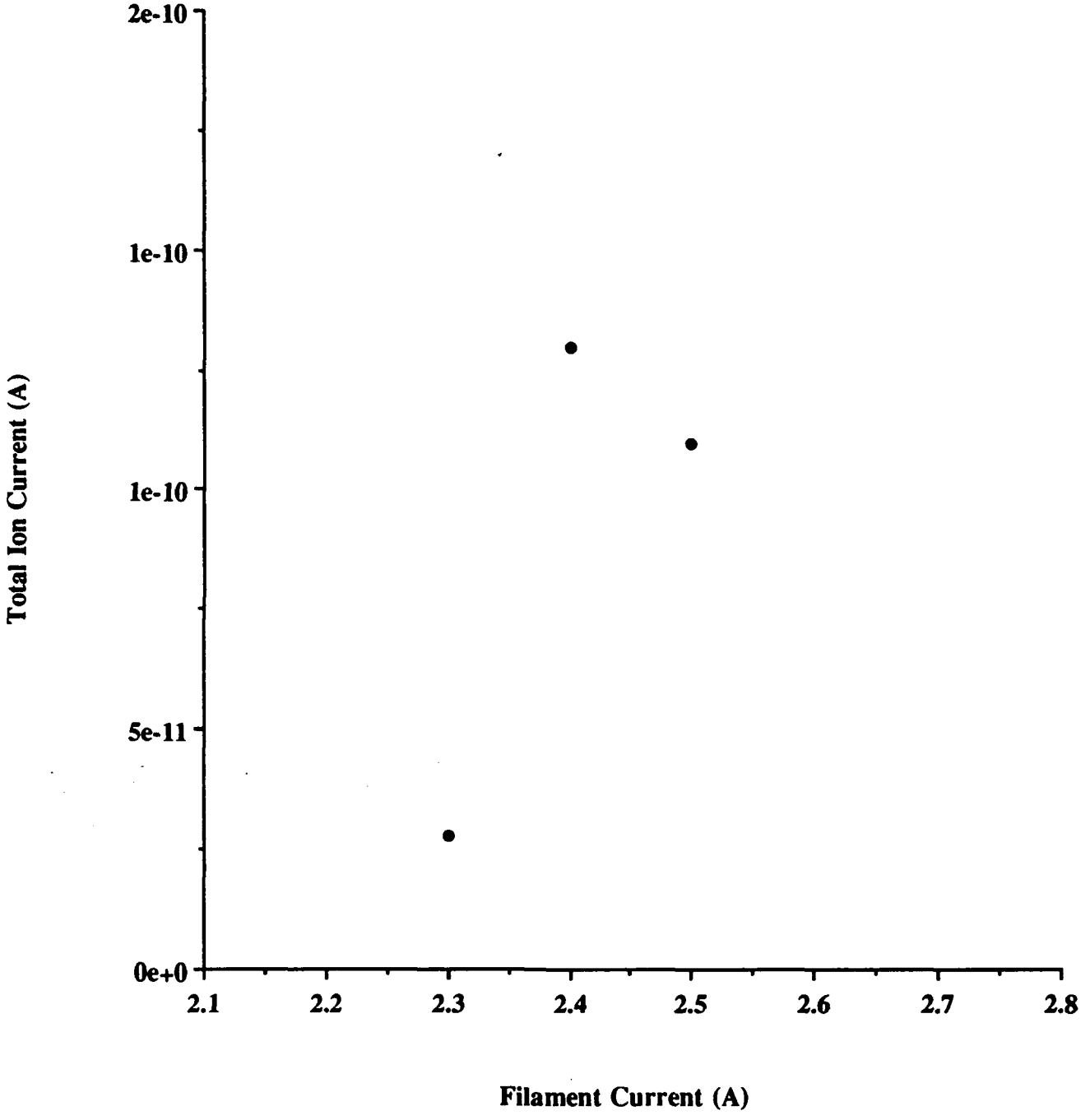

Figure 17. Total negative ion current as a function of filament current for sulfur hexafluoride at an ionization gauge pressure of 1 x 10^{-4} torr. Ion source configuration: I.V. = -15V; E.E. ~ 1 eV; X = 40V; F = 20V; R = -60V; C = +35V; with magnets.